ANNALI DI GEOFISICA, VOL. XXXVIII, N. 3-4, September-October 1995

Focal mechanism of seismic events with a dipolar component

Fausto Batini([1]), **Michele Caputo**([2]) **and Rodolfo Console**([3])
([1]) *ENEL, Unità Nazionale Geotermica, Larderello, Pisa, Italy*
([2]) *Università degli Studi «La Sapienza», Roma, Italy*
([3]) *Istituto Nazionale di Geofisica, Roma, Italy*

Abstract
In this paper we model the geometry of a seismic source as a dislocation occurring on an elemental flat fault in an arbitrary direction with respect to the fault plane. This implies the use of a fourth parameter in addition to the three usual ones describing a simple double couple mechanism. We applied the radiation pattern obtained from the theory to a computer code written for the inversion of the observation data (amplitudes and polarities of the first onsets recorded by a network of stations). It allows the determination of the fault mechanism generalized in the above mentioned way. The computer code was verified on synthetic data and then applied to real data recorded by the seismic network operated by the Ente Nazionale per l'Energia Elettrica (ENEL), monitoring the geothermal field of Larderello. The experimental data show that for some events the source mechanism exhibits a significant dipolar component. However, due to the high standard deviation of the amplitude data, *F*-test applied to the results of the analysis shows that only for two events the confidence level for the generalized model exceeds 90%.

Key words *microseismicity – fault mechanism – geothermal field*

1. Introduction

The most general point source is described by a moment tensor containing six independent components (Aki and Richards, 1980), which can be reduced to five if we consider only the geometry of the source (De Natale *et al.*, 1985; Julian, 1986, O'Connel and Johnson, 1988; Vasco, 1990). This model of a focal mechanism may, in general, have a volumetric (or isotropic) component, *i.e.* the trace of the tensor is not zero. Due to the difficulty of explaining such volumetric component, because of the large confining pressures at the depth where earthquakes occur, most of the focal mechanism solutions make the implicit use of the hypothesis that the trace of the moment tensor is null. In conjunction with the second hypothesis that also the determinant of the moment tensor is null, we have the most common mechanical model of an earthquake source: the double couple characterized by three free parameters (see *e.g.*, De Natale and Zollo, 1989). Still maintaining the hypothesis of a null trace we may introduce the Compensated Linear Vector Dipole (CLVD), either without any deviatoric component (two free parameters) or in conjunction with a parallel double couple (four free parameters) (see *e.g.*, Julian, 1983; Julian and Sipkin, 1985; Sipkin, 1986).

A volumetric component in the moment tensor describing earthquake sources observed in nature has been invoked more or less explicitly in literature, but it was not claimed as necessary by all the authors who considered the problem. All the observations in this sense

refer to areas subject to extensional stress regime such as volcanic and geothermal ones. «Anomalous» patterns of P first onsets with excess of compressional polarities, suggesting the presence of dipolar stress release, were observed by Klein *et al.* (1977) and by Einarsson (1979) for earthquakes occurred in the Middle Atlantic Ridge. Chouet (1979) reported about seismic surveys conducted around the Kilauea Iki crater, Hawaii. The first motion in the seismograms appeared to be always outward from the source, suggesting that a crack opening under tensile stress owing to cooling was the responsible source for the observed activity. Another possible interpretation of the data given by Chouet (1981) is the jerky opening of a channel connecting two fluid-filled cracks, owing to the excess pressure of fluid in one of the cracks. Foulger and Long (1984) and Foulger (1988) studied the microseismic activity of the Hengill geothermal area in the Neovolcanic Zone of Iceland. They observed that the far-field radiation pattern was predominantly compressional but a few dilatational arrivals were also observed. The predominant component of the inferred mechanism is a Linear Vector Dipole involving a volume increase. The dilatational part of the radiation field would be generated by a pore pressure drop caused by restricted fluid flow at the moment of fissuring. In this respect the source differs fundamentally from the CLVD source recognized by Julian (1983). De Natale and Zollo (1987) observed a significant isotropic component for one event recorded by a local seismic network in the volcanic region of Campi Flegrei (Southern Italy). Later on, the same authors (De Natale and Zollo, 1989) studying a set of 18 microearthquakes still occurred in the same volcanic region, concluded that the F-test did not allow to reject the hypothesis of simple double-couple mechanism for any of those events. O'Connel and Johnson (1988), in a study of three events recorded in the Geysers geothermal field, estimated large isotropic and CLVD components for one of them. However, they concluded that this substantial result could be explained by the unfavourable source-receiver geometry for this particular event.

2. Generalized model of an elemental flat dislocation

Usually the geometry of a double-couple source mechanism of an earthquake is modelled by a dislocation $\boldsymbol{u}$ on an elemental flat fault of area A in a direction *contained* on the fault plane itself (Aki and Richards, 1980). This source, equivalent to a pure deviatoric stress variation, is geometrically defined by three angles: two for identifying the fault plane (its strike ϕ and dip δ), and one for the rake λ on the fault. The determination of these angles requires normally the inversion of data recorded by a number of seismic stations. The data used for inversion are usually polarities of first onsets (P waves) recorded on seismograms or, more seldom, relative amplitudes of such onsets at the various stations (Shapira and Bath, 1978; De Natale *et al.*, 1985).

In this work we model the geometry of the seismic source by means of a dislocation occurring on an elemental flat fault in an *arbitrary* direction with respect to the fault plane itself. This implies the use of a fourth parameter, hereafter called θ, defined as the angle between the dislocation vector $\boldsymbol{u}$ and the fault plane. This source cannot be represented simply by a double couple, and consequently neither the determinant nor the trace of the equivalent moment tensor are constrained to zero. Nevertheless our model is different from the most general moment tensor because it implies one degree of freedom less than the latter.

As it was previously shown (Caputo and Console, 1989) the solution of the direct problem gives the radiation pattern of P and S waves for a generalized seismic source, including both shear and tensile dislocations. The formulas characterizing this solution are detailed in Appendix. The most remarkable feature of the radiation pattern of P waves for a similar source, in comparison with that of a simple double couple, is that in this more general case compressional and dilatational rays are not separated by orthogonal planes. For an opening crack ($\theta > 0^{\circ}$) the solid angle containing positive pulses is generally wider than that containing negative ones. Moreover, the average amplitude of the positive pulses is greater

than that of the negative ones. If θ exceeds a threshold value θ_c depending on the Lamé constants of the elastic medium ($\theta_c \cong 27°$ for $\lambda = \mu$) negative pulses are not observed at all and the whole P radiation pattern is characterized by positive pulses of variable amplitudes.

3. The algorithm for inversion

We prepared a computer code that allows the generalized focal mechanism to be determined from the displacement amplitudes of first P motion recorded by vertical component seismograph stations suitably disposed around the epicentral area. The method is the same developed by Shapira and Bath (1978) for a pure shear source, supposing the linear size of the source to be small in comparison with the distance from the nearest station. After correction for geometrical spreading, free surface effect and subsequent normalization, the recorded amplitudes are compared with those computed, iteratively changing the four parameters (ϕ, δ, λ, θ) fully characterizing the dislocation. The search for the best fit is conducted in two steps, starting from a coarse grid spanning all the possible ranges, and moving to a finer grid in smaller ranges around the best set of parameters found in the first step. The best fit for the four source parameters is reached by minimizing the standard deviation of the residuals between the theoretical and observed amplitudes. The basic input data necessary for performing the above mentioned algorithm are:

a) hypocentral coordinates of the source;

b) coordinates and elevation of the seismic stations;

c) velocity model of the crust in the concerned area;

d) amplitude and polarity of the first pulses measured on the seismograms;

e) magnification of each seismograph.

In order to test the new algorithms, we prepared a specific code for the solution of the direct problem, *i.e.* to obtain the values of amplitudes of the first arrival expected at the various stations, given their coordinates, together with the coordinates and the focal mechanism of the hypothetical source. This code gives, of course, the same results as that using the classic algorithm of a pure shear source with only three degrees of freedom, in the limit case of a dislocation parallel to the fault plane ($\theta = 0°$). The results obtained in the case of a pure volume source ($\theta = 90°$) can also be easily predicted and checked.

The tests were carried out on synthetic data obtained simulating real experimental environments. The source to be analyzed was located at five kms depth, in the first layer of a two-layer crust. The data were supposed collected by a network of twelve stations, almost evenly azimuthally distributed around the source, and with epicentral distance ranging from 3 to 19 km. In such circumstance, seven stations would receive direct waves and five refracted waves, as first arrivals.

The source parameters were assigned as follows: $\delta = 30°$, $\lambda = 45°$, $\phi = 15°$ with four different choices for θ ($\theta = 0°$, $10°$, $20°$ and $30°$). In the case of $\theta = 0°$, six stations would observe negative polarity and six would observe positive polarities for the first P wave pulse. Running the «direct» program, we obtained a set of synthetic data for each of the four cases not affected by experimental errors. By means of a simple algorithm we modified the synthetic observation data randomly, as they were affected by experimental errors of given standard deviations. Using such modified amplitudes in input, the inversion program gives, as expected, different results at each time, and in this way the stability of the method can be tested simulating various qualities of input data.

For each of the four sets of source parameters, we added to the normalized theoretical amplitudes random values with zero mean and the same standard deviation $\sigma = 0.01$ (one percent of the maximum amplitude). The standard deviation was then increased in five steps to 0.02, 0.05, 0.10, 0.20 and 0.50.

For each of the (24) above cases, the test was run ten times and the results were analyzed computing the averages of the source parameters so obtained, and their standard deviations. In total, each version of the algorithms (with four and three free parameters respectively) was tested with 240 different sets of input data.

The method provides excellent results in all cases with $\sigma = 0.01$ and $\sigma = 0.02$, when the algorithm with four free parameters is used. The results are also very good for $\sigma = 0.05$ and $\theta \leq 10^{\circ}$, and are still reliable for $\theta \geq 20^{\circ}$. The standard deviation of the solution parameters increases, in general, with the increase of the standard deviation of the input data. When the parameter θ is constrained to zero, on the contrary, there are good solutions only if the source model is characterized by $\theta = 0^{\circ}$ also. In this case, of course, there is not relevant difference with the results obtained by the four free parameter algorithm. As far as we increase the value of θ, therefore, increasing the normal component of the dislocation, the solution becomes more and more disturbed in the other three parameters, that are typical of a pure shear source.

Increasing σ to 0.10. we still obtain fairly good results using the algorithm of the general model with four free parameters. The standard deviation of θ is of the order of magnitude of a few degrees. Moving to $\sigma = 0.20$, the results are stable only for the parameter θ, which shows a standard deviation of a few degrees only. The case of $\sigma = 0.50$ brings to the completely random behaviour of the results concerning the three «pure shear» model parameters. Nevertheless, the values of the fourth parameter θ are still consistent with those of the given model at least for $\theta \leq 10^{\circ}$, and affected by a standard deviation not exceeding 10° even in the worst case. A systematic reduction is noted in the values of θ for the results of the inversion program with respect to those of the source model for $\theta \geq 20^{\circ}$. However, we could note that the average value of the standard deviation of the residuals obtained from the four parameter algorithm for $\theta \geq 10^{\circ}$, even in the case of $\sigma = 0.50$, is less than the corresponding values obtained by the algorithm with θ constrained to zero, and no errors on the input data.

4. Application to real data

The algorithm briefly described in the previous section was applied to data recorded by the 26 stations of the ENEL seismological network deployed in the geothermal field of Larderello, Central Italy (fig. 1) (Batini *et al.*, 1980, 1985). The geometry of this network was optimized according to the topological criteria of Caputo (1978). Each station is equipped with a vertical seismometer type S-13 characterized by 1 s free period and generator constant of 620 V/m/s. The seismic signals, amplified and frequency modulated, are transmitted by radio links where they are recorded on a digital acquisition system with a sampling rate of 250 sps after anti-aliasing filtering at 48 Hz.

We analyzed 19 microearthquakes occurred between January and April, 1988 (table I). Their M_l magnitude ranged between 0.4 and 1.6 and they were recorded by a minimum number of 13 to a maximum of 24 stations within an epicentral distance of 30 km (fig. 1). The focal depth ranged from less than 3 km to 11 km. Figure 2 gives an indication of the data quality. All the hypocentral parameters listed in table I were computed by routine procedures at the ENEL data center of Larderello, using the Hypoellipse code (Lahr, 1979). The velocity model of the crust is represented by flat layers (different from one station to another) and was determined on the basis of geologic (stratigraphy of wells) as well as geophysical (seismic exploration, sonic logs) information. Typically, the *P*-velocity models include one or two layers some tens of meters thick at low velocity (3-4 km/s), one layer 3-4 km thick at 5.1 km/s, and a basement of 6.2 km/s.

The last two columns in table I indicate the number of stations reporting data for each event and the maximum azimuthal gap between stations. The latter parameter is related to the position of the epicenter inside the network of stations and gives an indication of the reliability of our focal mechanism solution. In fact, a good solution strongly depends on a homogeneous distribution of stations around the epicenter. The present set of events was selected from a larger one retaining all (and only) those for which the azimuthal gap was less than 90°.

In table II two sets of solutions obtained for the focal mechanism of the same 19 events are reported. The first set concerns the solutions

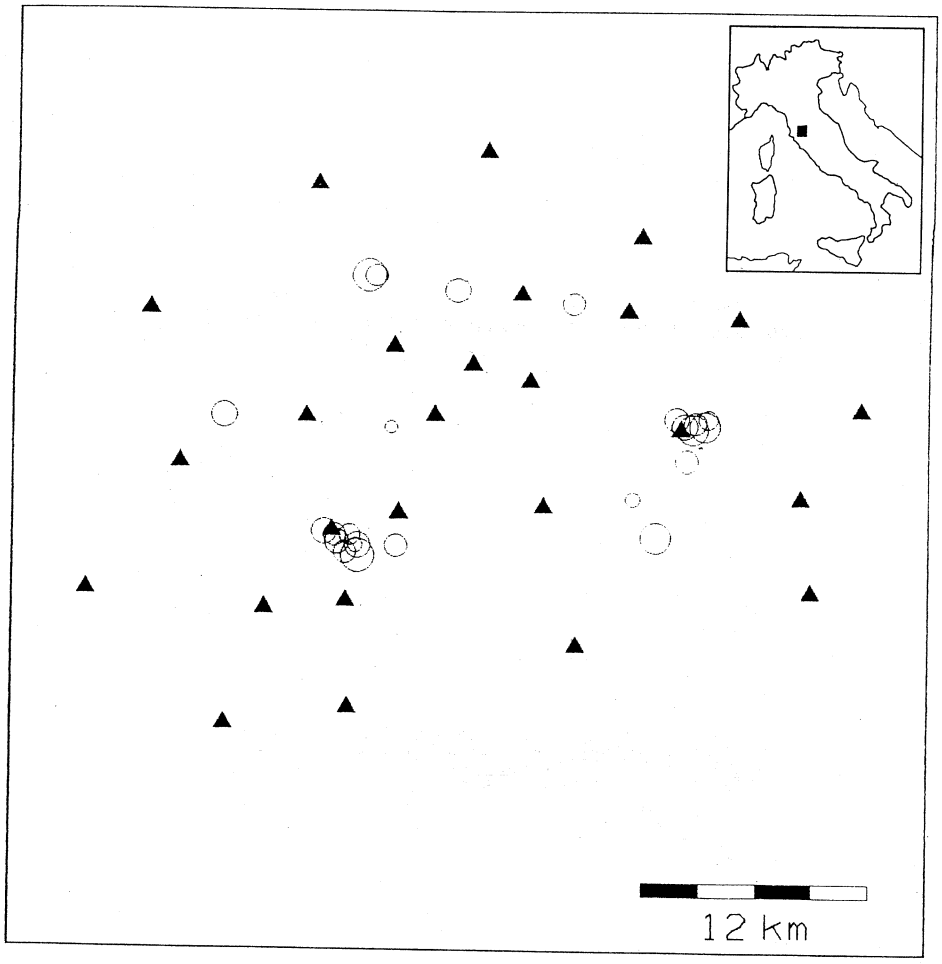

Fig. 1. Map of the seismic stations of the network operated by ENEL in the geothermal field of Larderello (black triangles), and epicenters of the events analyzed in this study (open circles). The size of the circles is proportional to the magnitude of the events.

obtained using a pure double-couple model and contains only three parameters: the strike ϕ, the dip δ, and the rake λ. The second set concerns the solutions obtained by the generalized model and includes the fourth parameter θ. In both sets σ is the standard deviation of the amplitude residuals scaled to the maximum amplitude. As expected, σ is *always* smaller for the 4-parameter solution than for the 3-parameter solution, because of the higher number of parameters found in the solution.

It is interesting to make a comparison between the two sets of solutions. Three events (No. 5, 11, 13) achieve a small value for θ. Of course in this case the values of the three parameters ϕ, δ and λ, and also that of the standard deviation σ, are very similar between the two solutions of each event. It probably means that the double-couple model is applicable to such events.

Of the remaining 16 events, only one (No. 18) presents a negative value of θ, that

Table I. List of the events analyzed in this study.

Event	Date	Time	Lat. (N)	Long. (E)	Depth (km)	M_l	N_{st}	Gap (°)
1	12/1/88	04:29	43°08.6'	10°51.1'	4.2	1.0	16	78
2	15/1/88	12:37	43°08.7'	10°48.8'	5.9	1.1	15	57
3	15/1/88	12:59	43°08.4'	10°49.1'	3.2	1.0	20	68
4	27/2/88	05:45	43°08.9'	10°48.7'	5.0	1.0	14	61
5	4/4/88	08:29	43°12.1'	11°02.4'	9.6	1.2	16	63
6	6/4/88	19:24	43°11.1'	11°02.5'	11.3	1.0	17	73
7	22/4/88	11:38	43°16.0'	10°53.4'	6.1	1.2	23	64
8	10/6/88	09:01	43°12.3'	11°03.3'	3.8	0.8	23	71
9	10/6/88	09:02	43°12.5'	10°03.3'	3.9	1.0	24	73
10	4/8/88	06:53	43°12.0'	10°50.9'	3.1	0.4	18	81
11	17/9/88	20:46	43°15.6'	10°58.0'	6.5	1.1	23	75
12	30/9/88	17:12	43°10.0'	11°00.4'	2.5	0.5	20	84
13	14/10/88	20:15	43°08.9'	10°49.3'	3.9	0.9	23	66
14	18/10/88	14:23	43°12.3'	11°02.1'	2.6	1.1	23	57
15	8/4/89	00:44	43°08.6'	10°49.6'	4.1	1.2	21	70
16	29/7/89	12:57	43°09.0'	10°48.3'	3.3	1.2	18	59
17	9/10/89	21:46	43°08.6'	10°49.5'	3.5	0.5	13	69
18	27/11/89	23:43	43°12.1'	11°03.2'	3.9	1.5	18	83
19	27/11/89	23:45	43°12.0'	11°02.7'	4.0	1.5	18	85

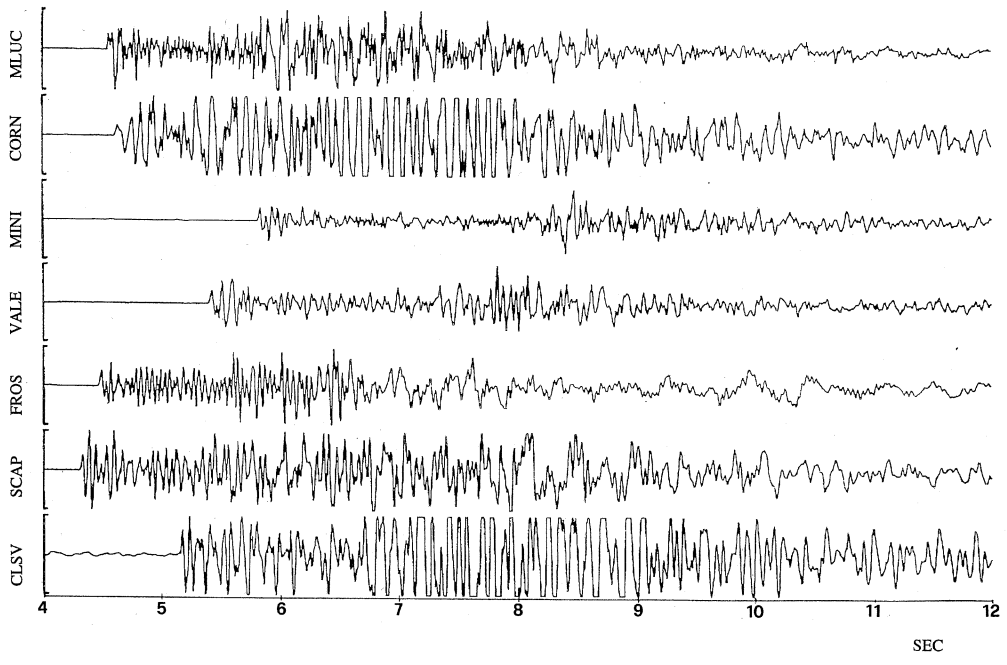

Fig. 2. Seismograms of the event No. 9 recorded by the ENEL seismological network in the geothermal field of Larderello.

Table II. Source parameters.

Event	3-parameter solution				4-parameter solution				
	ϕ	δ	λ	σ	ϕ	δ	λ	θ	σ
1	−81	−11	60	0.222	−87	−5	72	15	0.174
2	90	17	−82	0.320	−90	79	−78	9	0.267
3	−22	65	−17	0.335	−68	43	−72	13	0.228
4	2	86	87	0.337	10	−3	−90	12	0.224
5	−63	35	−85	0.268	−60	34	−83	−1	0.266
6	−82	−74	49	0.414	−29	30	−81	13	0.384
7	−51	−90	−61	0.345	−52	−59	−35	18	0.311
8	−23	17	−57	0.329	72	−47	−77	24	0.296
9	−19	13	−73	0.328	8	14	−7	10	0.290
10	−10	40	90	0.373	56	−63	−77	24	0.296
11	−77	−83	−78	0.321	−75	−79	−78	4	0.311
12	17	−35	−90	0.470	2	−43	−74	9	0.423
13	−88	32	−50	0.257	−87	33	−48	1	0.256
14	39	−60	27	0.328	−15	25	86	18	0.250
15	−78	17	−62	0.355	66	−90	65	15	0.283
16	−54	−44	90	0.496	77	29	−82	17	0.413
17	−45	87	89	0.200	−20	−7	−90	9	0.108
18	84	−29	45	0.277	−79	48	−90	−9	0.243
19	90	−27	58	0.268	78	−35	28	11	0.263

suggests a closing crack mechanism, obviously occurring in a pre-existing opened crack, but the small reduction on σ leads us to consider this solution unreliable. All the other 15 events present a positive value of θ ranging from 9 to 24 degrees (suggesting an opening crack mechanism).

Figures 3 to 5 show the lower hemisphere stereographic projection of the focal mechanism for three of the analyzed microearthquakes. Both the double couple and the generalized solutions are drawn for comparison. In these figures, not only polarities, but also relative amplitudes of the first P onsets, are reported.

We should remark that the first pulses recorded at many stations for the stronger events, since their amplitude was larger than the saturation level, were clipped.

Table III shows the number of dilatational, nodal, and compressional P-wave polarities observed for each of the analyzed events. These numbers are indicated by N_D, N_N and N_C respectively. An excess of compressional polarities is expected for focal mechanisms including isotropic component.

Making use of tables I and II, one can judge about the reliability of the focal mechanism solutions. For example, the event No. 4 (fig. 4) was recorded with an azimuthal gap of only 61° and the 4-parameter solution is characterized by a standard deviation 30% smaller than the 3-parameter solution. It suggests the validity of the hypothesis of a tensional crack in this case.

The Gauss criterion provides a simple way to establish the relative goodness of two hypothesis fitting the same set of experimental data. It is expressed by

$$R_{\mathrm{m}} = \sum_{1}^{n}{}_{i} r_i^2 / (n - m) = \text{minimum}$$

where r_i is the residual of the i-th measurement, n is the number of experimental points to be fitted and m is the number of parameters to be determined in the inversion of the formulae. The quantity $(n\text{-}m)$ is generally called number

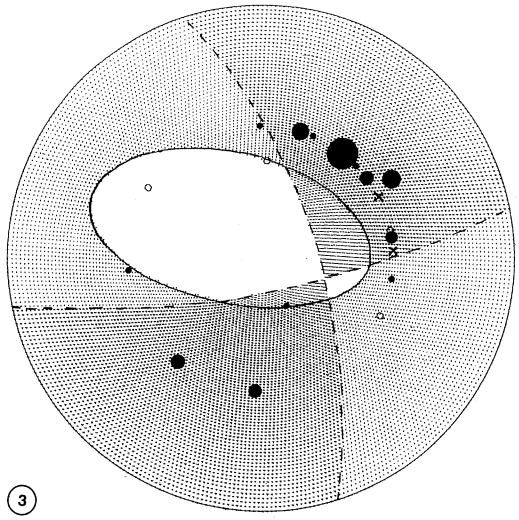

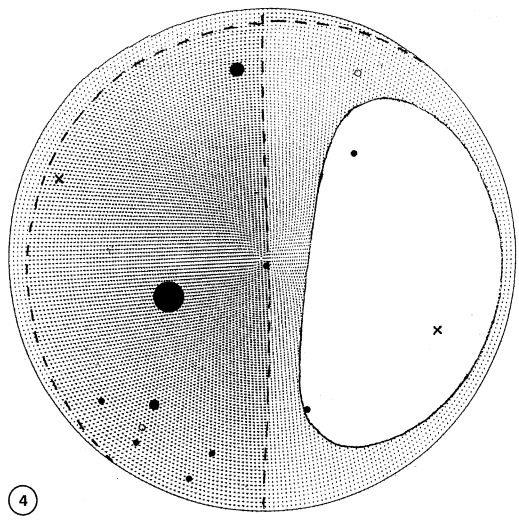

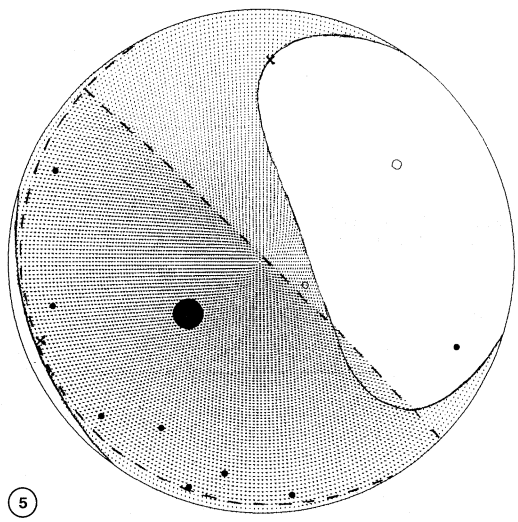

Fig. 3. Lower hemisphere stereographic projection of the focal sphere for the event No. 3 analyzed in this study. Station *P* pulses are indicated by circles (white for dilatational onsets and black for compressional ones). Nodal arrivals are represented by crosses. The size of the circles is scaled to the measured amplitude corrected for geometrical spreading and free space effect. Nodal planes for double-couple solution are represented by dashed lines. Nodal surfaces for the generalized solution are represented by full lines.

Fig. 4. Same as fig. 2 for event No. 4.

Fig. 5. Same as fig. 2 for event No. 17.

of degrees of freedom. Table III shows the values of R_m obtained by the 3-parameter and 4-parameter model respectively. For example, for the event No. 4 we obtained $R_3 = 0.1445$ and $R_4 = 0.0702$, which seem to confirm the validity of the second hypothesis. The same comments apply to events No. 1, 3, 14, 15 and 17.

The Gauss test alone does not tell us the reliability of the choice between two hypotheses. To have a quantitative estimate of the reliability, more robust statistics must be used. It is done through the Fisher test that compares the ratios of the variances obtained by the two models ($F_{3,4} = R_3/R_4$) with tabled values (F_0) related to the selected confidence level taking into account the number of degrees of freedom. The last two columns of table III show the results of the *F*-test applied to our data for a confidence level of 90%. The results are positive only for two of the analyzed events (No. 3

Table III. Statistical tests.

Event	N_D	N_N	N_C	Gauss test		Fisher test	
				R_3	R_4	$F_{3,4}$	F_0
1	0	0	16	0.0606	0.0404	1.50	2.10
2	4	2	9	0.1182	0.0972	1.32	2.21
3	4	2	14	0.1320	0.0650	2.03	1.89
4	5	0	9	0.1445	0.0702	2.06	2.28
5	3	6	7	0.0884	0.0943	0.94	2.10
6	6	1	10	0.2081	0.1928	1.08	2.01
7	3	2	18	0.1369	0.1170	1.17	1.81
8	4	2	17	0.1245	0.1061	1.81	2.16
9	3	1	19	0.1230	0.0961	1.22	1.79
10	8	5	5	0.1670	0.1126	1.10	2.01
11	3	0	20	0.1185	0.1172	1.01	1.81
12	9	4	7	0.2599	0.2238	1.16	1.89
13	6	3	14	0.0757	0.0790	0.96	1.81
14	11	2	10	0.1237	0.0756	1.64	1.81
15	3	0	18	0.1470	0.0994	1.49	1.86
16	4	0	14	0.2958	0.2196	1.35	2.01
17	2	2	9	0.0518	0.0167	3.08	2.42
18	7	4	7	0.0918	0.0759	1.17	2.42
19	3	2	13	0.0862	0.0889	1.00	2.01

and 17). It means that for these events there is a probability greater than 90% that the improvement in the standard deviation of the 4-parameter model with respect to the 3-parameter model is not just a consequence of statistical fluctuations.

The circumstance that for only two events the data have shown the validity of the model with a dipolar component could appear deluding in some way. An explanation of such circumstance can be found in the high level of noise which affects experimental data. Figures 3 to 5 show that there is a relevant scattering in the amplitudes recorded at sites close to each other. It is, in fact, well known that the use of first pulses amplitudes is a delicate matter: beside the radiation pattern there is to be taken into account the influence of local site amplification and, even more important in geothermal areas, of attenuation properties. By means of simulations carried out on synthetic data we could establish that a mechanism with tensional component $\theta = 5^\circ$ can be appreciated at a confidence level of 90% if the standard deviation on the normalized amplitudes is less than 0.1. A standard deviation greater than 0.2, usually met in our data, constitutes a serious problem for the estimate of a tensional component smaller than 10°.

The F-test, carried out on single solutions, does not allow to reject the hypothesis of double couple solution for any of the 19 events at a significance level better than 95%, and only for two of them at the 90% level. This result is similar to that reported by De Natale and Zollo (1989). However, the evident bias of values obtained for θ (positive for 17 events out of 19) shown in table III, does not seem to come from a random distribution. This is in connection with the significant excess of compressional polarities in the data set available for this study. Taking into consideration the fact that this data set comes from an unbiased selection of events whose epicenters are distributed over the whole monitored area, it suggests the existence of a dipolar component for a significant fraction of the events (see also, Chouet, 1979; Foulger, 1988).

5. Conclusions

We developed a method of analysis for focal mechanisms taking into account a component of the dislocation normal to the fault plane (dipolar component) related to the increase of the source volume as in the case, *e.g.*, of a tensional crack opening.

At least 6 (32%) of the microearthquakes analyzed in this study, and occurred in the geothermal field of Larderello, exhibit a focal mechanism with a large component of dislocation normal to the fault plane. For two of these events the *F*-test confirms the validity of this model with a confidence level greater than 90%. The relevant noise level in the observation data, mostly due to the lack of a suitable attenuation model, puts a limit to the statistical significance of the hypothesis based on a mechanism more complex than that of a single double couple. However, the strong excess of compressional polarity in the overall database, for a set of earthquakes sparsely distributed in the area monitored by the network, indicates the existence of an isotropic component at least for a part of the events.

The investigation on a more comprehensive set of data and the use of a propagation model more complex than a simple half-space could lead to more reliable results. A correlation between the geographic position of the epicenters and the various mechanisms of fracturing, would improve our knowledge of the stress field in the area and of its attitude to be geothermally exploited.

Acknowledgements

Dr. Rosa Rosini developed the algorithms of the *F*-test. The suggestions given by the anonymous reviewer greatly contributed to the improvement of the manuscript.

Appendix

The n component of the displacement $\boldsymbol{u}$ caused in P by a point source, in the origin of the coordinates, with moment tensor M_{pq} is obtained (Aki and Richards, 1980) from the convolution

$$u_n = M_{qp} * G_{nq,p} \tag{A.1}$$

where G_{nq} is the Green function for a point force in the direction of the axis x_p. M_{qp} are the components of the moment tensor

$$M_{pq} = \int_\Sigma \int m_{pq}\, d\Sigma = \int_\Sigma \int (\lambda \nu_k\, [u_k]\, \delta_{pq} + \mu\, [\nu_p u_q + \nu_q u_p])\, d\Sigma \tag{A.2}$$

where m_{pq} is the moment tensor density, ν_k are the components of the normal to the surface Σ where the dislocation occurred, λ and μ are the elastic parameters and $[u_i]$ are the components of the dislocation on Σ.

For the far field in a homogeneous medium, the Green function can be written explicitly and from (A.1), for an elementary fault of area A, we obtain

$$\begin{aligned} u_n = {} & A/(4\pi\rho\alpha^3 r)\, [\lambda\, \gamma_n\, \nu_k\, u_k + 2\mu\, \gamma_n\, \gamma_p\, \gamma_q\, \nu_q\, u_p] + \\ & -\mu A / (4\pi\beta^3 r)\, [2\, \gamma_n\, \gamma_q\, \nu_q\, \gamma_p\, u_p - \gamma_p\, \nu_n\, u_p - \delta_{np}\, \gamma_q\, \nu_q\, u_p], \end{aligned} \tag{A.3}$$

where γ_i are the components of the unit vector in the direction from the source to the receiver separated by the distance r, α and β are the velocities of the P and S waves, and the expressions in square brackets are computed at the delayed time $t\text{-}r/\alpha$ and $t\text{-}r/\beta$ respectively.

Let us now transfer the components of $\boldsymbol{u}$, which are in the x_1, x_2, x_3 system of the source, into the $\boldsymbol{r}$, θ, ϕ coordinate system of the station in P, $\boldsymbol{r}$ being the unit vector in the direction of the ray in P, θ perpendicular to $\boldsymbol{r}$ in the vertical plane, positive from $\boldsymbol{x}_3$, ϕ perpendicular to $\boldsymbol{r}$ and θ, positive counter-clockwise; the fault is in the origin of the x_1, x_2, x_3 coordinates and in the plane x_1, x_2; the slip $\boldsymbol{u}$ may not be in the plane of the

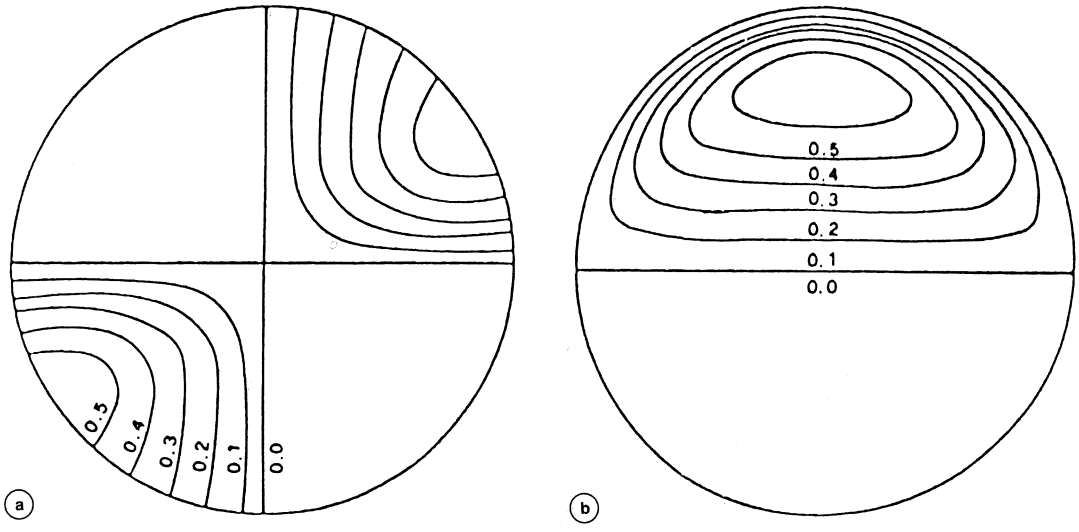

Fig. A1a,b. Nodal lines in the lower hemisphere projection for (a) a strike slip fault and (b) dip slip fault, for a mechanism with dipolar component, shown for different values of $\mathrm{tg}\,\theta$.

fault; we take it in the most general direction, rotating the reference frame around x_3 to contain it in the plane x_1, x_3: $\boldsymbol{u} = u_1\, x_1 = u_3\, x_3$.

The only nonzero component due to the P wave at the station is in the $\boldsymbol{r}$ direction; it is

$$\mu A/(4\,\pi\rho\alpha^3 r)\;[\lambda/\mu\, u_3 + 2\,(u_1\,\sin\theta\cos\phi + u_3\cos\theta)\cos\theta]\;\boldsymbol{r}\,; \tag{A.4}$$

while the non nil components due to the S wave at the station are

$$\mu A/(4\,\pi\rho\beta^3 r)\;[u_1\,(\cos\phi\cos 2\theta\,\theta - \cos\theta\,\sin\phi\,\phi) - u_3\,\sin\theta\,\cos\theta\,\theta]\,. \tag{A.5}$$

The $\boldsymbol{r}$ component due to the S wave is nil, and the θ and ϕ components give the S radiation pattern.

In order to be able to use the formulas obtained above, we shall express them as functions of the angles describing the directions of the source plane and of the slip, which are the unknowns of the problem to be estimated from the recording of the signals at the stations around the source.

Carrying out the computations, we obtain the radiation patterns for the P, SV and SH waves (Caputo and Console, 1989):

$$\begin{aligned}
\mathcal{F}P = {} & \{\cos\lambda\,\sin\delta\,\sin^2 i_\xi\,\sin 2(\phi-\phi_s) - \cos\lambda\,\cos\delta\,\sin 2i_\xi\,\cos(\phi-\phi_s) + \\
& + \sin\lambda\,\sin 2\delta\,[\cos^2 i_\xi - \sin^2(\phi-\phi_s)\sin^2 i_\xi] + \\
& + \sin\lambda\,\cos 2\delta\,\sin 2i_\xi\,\sin(\phi-\phi_s)\}\cos\theta + \\
& \{\lambda/\mu + 2\,[\sin i_\xi\,\sin\delta\,\sin(\phi-\phi_s) - \cos\delta\,\cos i_\xi]^2\}\sin\theta\,, \\
\mathcal{F}SV = {} & \{\sin\lambda\,\cos 2\delta\,\cos 2i_\xi\,\sin 2(\phi-\phi_s) - \cos\lambda\,\cos\delta\,\sin 2i_\xi\,\cos(\phi-\phi_s) + \\
& + 1/2\,\cos\lambda\,\sin 2\delta\,\sin 2i_\xi\,\sin 2(\phi-\phi_s) + \\
& - 1/2\,\sin\lambda\,\sin 2\delta\,\sin 2i_\xi\,[1+\sin^2(\phi-\phi_s)]\}\cos\theta + \\
& + \{\sin 2\delta\,\cos 2i_\xi\,\sin(\phi-\phi_s) + \sin 2i_\xi\,[\sin^2\delta\,\sin^2(\phi-\phi_s) - \cos^2\delta]\}\sin\theta\,, \\
\mathcal{F}SH = {} & [\cos\lambda\,\cos\delta\,\cos i_\xi\,\sin(\phi-\phi_s) + \cos\lambda\,\sin\delta\,\sin i_\xi\,\cos 2(\phi-\phi_s) + \\
& + \sin\lambda\,\cos 2\delta\,\cos i_\xi\,\cos(\phi-\phi_s) - 1/2\,\sin\lambda\,\sin\delta\,\sin i_\xi\,\sin 2(\phi-\phi_s)]\cos\theta + \\
& + 2\,\sin^2\delta\,\cos^2(\phi-\phi_s)\sin\theta\,,
\end{aligned} \tag{A.6}$$

where ϕ_s, δ and λ are respectively the strike, dip angle and rake of the fault; θ is again the angle between the fault plane and the slip vector; ϕ and i_ξ are the azimuth and the take off angle of the seismic ray. The case of $\theta = 0$ obviously reproduces the pure double couple source (Aky and Richards, 1980, page 115). Figure A1a,b shows examples of the nodal lines of the P wave radiation pattern in the lower hemisphere stereographic projection.

REFERENCES

AKI, R. and P. RICHARDS (1980): *Quantitative Seismology* (W.H. Freeman and Co., San Francisco).

BATINI, F., C. BUFE, G.M. CAMELI, R. CONSOLE and A. FIORDELISI (1980): Seismic monitoring in Italian geothermal areas. 1. Seismic activity in the Larderello-Travale region, in *Second DOE-ENEL Workshop for Cooperative Research in Geothermal Energy*, 20-23 October, Berkeley, California, U.S.A.

BATINI, F., R. CONSOLE and G. LUONGO (1985): Seismological study of Larderello-Travale geothermal area, *Geothermics*, vol. 14 (2/3), 255-272.

CAPUTO, M. (1978): Topology and detection capability of seismic networks, in *Terrestrial and Space Techniques in Earthquake Prediction Research*, edited by A. VOGEL (Friedr. Vieweg Son, Braunschweigh/Wiesbaden).

CAPUTO, M. and R. CONSOLE (1989): Seismic inversion for a crack opening, in *Atti Acc. Naz. Lincei, Rend. Fis.*, **82** (8), 757-771.

CHOUET, B. (1979): Sources of seismic events in the cooling lava lake of Kilauea Iki, Hawaii. *J. Geophys. Res.*, **84**, 2315-2330.

CHOUET, B. (1981): Ground motion in the near field of a fluid-driven crack and its interpretation in the study of shallow volcanic tremor, *J. Geophys. Res.*, **86**, 5985-6016.

DE NATALE, G., G. IANNACCONE and A. ZOLLO (1985): Un metodo per la determinazione del meccanismo focale del tensore momento, in *Atti IV Convegno GNGTS*, CNR, Roma.

DE NATALE, G. and A. ZOLLO (1987): Parametri di sorgente sismica e caratteristiche del mezzo di propagazione ai Campi Flegrei dedotti dall'analisi di dati da una rete sismica digitale a 3 componenti, in *Aree Sismogenetiche e Rischio Sismico in Italia* – I, edited by E. BOSCHI and M. DRAGONI (Il Cigno Galileo Galilei, Roma).

DE NATALE, G. and A. ZOLLO (1989): Earthquake focal mechanisms from inversion of first P and S wave motions, in *Digital Seismology and Fine Modeling of the Lithosphere*, edited by R. CASSINIS, G. NOLET and G.F. PANZA (Plenum Press, New York).

EINARSSON, P. (1979): Seismicity and earthquake focal mechanisms along the mid-Atlantic plate boundary between Iceland and the Azores, *Tectonophysics*, **55**, 127-153.

FOULGER, G.R. (1988): Hengill triple junction, SW Iceland. 2. Anomalous earthquake focal mechanisms and applications for processes within the geothermal reservoir and at accretionary plate boundaries. *J. Geophys. Res.*, **93** (B11), 13507-13523.

FOULGER, G.R. and R.E. LONG (1984): Anomalous focal mechanisms: tensile crack formation on an accreting plate boundary, *Nature*, **310**, 43-45.

JULIAN, B.R. (1983): Evidence for dyke intrusion earthquake mechanisms near Long Valley Caldera, California, *Nature*, **303**, 323-325.

JULIAN, B.R. (1986): Analyzing seismic-source mechanism by linear programming methods, *Geophys. J. R. Astron. Soc.*, **84**, 431-443.

JULIAN, B.R. and S.A. SIPKIN (1985): Earthquake processes in the Long Valley Caldera Area, California, *J. Geophys. Res.*, **90**, 11155-11169.

KLEIN, F.W., P. EINARSSON and M. WYSS (1977): The Reykjanes peninsula, Iceland, earthquake swarm of September 1972 and its tectonic significance, *J. Geophys. Res.*, **82**, 865-888.

LAHR, J.C. (1979): Hypoellipse: a computer program for determining local earthquakes hypocentral parameters, magnitude and first motion pattern. Open-file Report U.S.G.S., Menlo Park.

O'CONNELL, D.R.H. and L.R. JOHNSON (1988): Second-order moment tensor of microearthquakes at The Geysers geothermal field, California, *Bull. Seism. Soc. Am.*, **78**, 1674-1692.

SHAPIRA, A. and M. BATH (1978): Source mechanism determination of short distance microearthquakes, *Seismological Institute*, Uppsala, Report No. 1-78.

SIPKIN, S.A. (1986): Interpretation of non-double-couple earthquake mechanisms derived from moment tensor inversion, *J. Geophys. Res.*, **91**, 531-547.

VASCO, D.W. (1990): Moment-tensor invariants: searching for non-double-couple earthquakes, *Bull. Seism. Soc. Am.*, **80**, 354-371.

(received February 20, 1995;
accepted October 6, 1995)